INFECTION AND IMMUNITY, Sept. 2010, p. 3861–3870 Vol. 78, No. 9
0019-9567/10/$12.00 doi:10.1128/IAI.00111-10
Copyright © 2010, American Society for Microbiology. All Rights Reserved.

Immunomodulatory Effects of Serotype B Glucuronoxylomannan from *Cryptococcus gattii* Correlate with Polysaccharide Diameter▽

Fernanda L. Fonseca,[1]† Lilian L. Nohara,[2]† Radames J. B. Cordero,[3] Susana Frases,[5] Arturo Casadevall,[3,4] Igor C. Almeida,[2]‡ Leonardo Nimrichter,[1]‡ and Marcio L. Rodrigues[1]*‡

Laboratório de Estudos Integrados em Bioquímica Microbiana, Instituto de Microbiologia Professor Paulo de Góes, Rio de Janeiro, RJ 21941-902,[1] and Laboratório de Biotecnologia, Instituto Nacional de Metrologia, Normalização e Qualidade Industrial, Rio de Janeiro, RJ 25250-020,[5] Brazil; Border Biomedical Research Center, Department of Biological Sciences, University of Texas at El Paso, El Paso, Texas 79968[2]; and Department of Medicine[3] and Department of Microbiology and Immunology,[4] Albert Einstein College of Medicine, 1300 Morris Park Avenue, Bronx, New York 10461

Received 2 February 2010/Returned for modification 9 March 2010/Accepted 9 June 2010

Glucuronoxylomannan (GXM), the major capsular component in the *Cryptococcus* complex, interacts with the immune system in multiple ways, which include the activation of Toll-like receptors (TLRs) and the modulation of nitric oxide (NO) production by phagocytes. In this study, we analyzed several structural parameters of GXM samples from *Cryptococcus neoformans* (serotypes A and D) and *Cryptococcus gattii* (serotypes B and C) and correlated them with the production of NO by phagocytes and the activation of TLRs. GXM fractions were differentially recognized by TLR2/TLR1 (TLR2/1) and TLR2/6 heterodimers expressed on TLR-transfected HEK293A cells. Higher NF-κB luciferase reporter activity induced by GXM was observed in cells expressing TLR2/1 than in cells transfected with TLR2/6 constructs. A serotype B GXM from *C. gattii* was the most effective polysaccharide fraction activating the TLR-mediated response. This serotype B polysaccharide, which was also highly efficient at eliciting the production of NO by macrophages, was similar to the other GXM samples in monosaccharide composition, zeta potential, and electrophoretic mobility. However, immunofluorescence with four different monoclonal antibodies and dynamic light-scattering analysis revealed that the serotype B GXM showed particularities in serological reactivity and had the smallest effective diameter among the GXM samples analyzed in this study. Fractionation of additional serotype B GXMs, followed by exposure of these fractions to macrophages, revealed a correlation between NO production and reduced effective diameters. Our results demonstrate a great functional diversity in GXM samples from different isolates and establish their abilities to differentially activate cellular responses. We propose that serological properties as well as physical chemical parameters, such as the diameter of polysaccharide molecules, may potentially influence the inflammatory response against *Cryptococcus* spp. and may contribute to the differences in granulomatous inflammation between cryptococcal species.

Cryptococcus neoformans and *Crptococcus gattii* are the etiologic agents of the human and animal fungal disease cryptococcosis. Infection is usually acquired by inhalation of environmental basidiospores or desiccated yeasts. Cryptococcal disease in humans can involve every tissue, including cutaneous and pulmonary sites, but the most serious manifestation is central nervous system involvement with meningoencephalitis (43). Despite the similarities of the clinical syndromes in cryptococcosis caused by *C. neoformans* and *C. gattii*, these species differ in the types of hosts in which they cause disease. While *C. neoformans* preferentially causes disease in immunosuppressed patients, *C. gattii*-related disease is relatively common in immunocompetent individuals (33, 43, 48). Mortality rates are still high in different regions of the globe, and the current therapeutic options are inefficient (1). No vaccines for the prevention of cryptococcosis are available.

Glucuronoxylomannan (GXM) is the major component of the polysaccharide capsule, which is the main virulence factor of *Cryptococcus* species (30). GXM is an anionic polysaccharide consisting of a α1-3-linked mannan that is O acetylated at carbon 6 of some of the mannosyl units and substituted with β1,2 glucuronyl and β1,2/β1,4 xylosyl residues (9). The polysaccharide is a capsular component of *Cryptococcus* species that is also abundant in its soluble form in culture fluids and infected tissues (31). Secreted and surface-associated forms of GXM are believed to modulate the immune response during cryptococcosis through multiple mechanisms (35). In addition, administration of monoclonal antibodies (MAbs) against GXM can modify the course of experimental cryptococcosis by prolonging host survival (3). Four serotypes of GXM (A to D) have been defined by serological reactions. This classification divides pathogenic *Cryptococcus* species into specific serotypes, such that *C. gattii* consists of serotypes B and C isolates, while *Cryptococcus neoformans* var. *grubii* and *Cryptococcus neoformans* var. *neoformans* correspond to serotypes A and D, respectively (23, 43). Most studies on the immunological functions of GXM have focused on the polysaccharide fractions from *C. neoformans* serotype A isolates. Although it is generally assumed that the immunological properties observed for

* Corresponding author. Mailing address: Avenida Carlos Chagas Filho 373, CCS, Bloco I. Instituto de Microbiologia, UFRJ, Rio de Janeiro, RJ, Brazil, 21941-902. Phone: 55 21 2598 3035. Fax: 55 21 2560 8344. E-mail: marcio@micro.ufrj.br.

† F.L.F. and L.L.N. contributed equally to this work.

‡ I.C.A., L.N., and M.L.R. share senior authorship of this article.

▽ Published ahead of print on 14 June 2010.

the serotype A polysaccharide are applicable to the other serological groups, this common assumption may not be correct, given the major structural differences among the four major serotypes.

The ability of GXM to activate the innate immune response has been reported in several studies (34, 46, 52, 53). Serotype A GXM has been reported to modulate the production of nitric oxide (NO) by phagocytes (5). In addition, GXM activates Toll-like receptor 4 (TLR4)-mediated intracellular signaling (46), but the contribution of this event to the global innate response against *C. neoformans* infections is uncertain (2, 39). GXM can also interact with TLR2 (46), which is believed to influence the response to cryptococcal infection (53). TLR2 recognizes a diverse set of pathogen-associated molecular patterns, and this recognition may require heterodimerization with TLR1 or TLR6 (14, 17, 22, 29, 50). The roles of TLR1 and TLR6 in the recognition of GXM by TLR2 have not been investigated yet.

In this study, we correlated the structural and physical chemical properties of five GXM samples with their abilities to stimulate NO production by macrophages and to activate nuclear factor κB (NF-κB) in cells expressing either TLR2/TLR1 (TLR2/1) or TLR2/TLR6 (TLR2/6). Our results demonstrate that a serotype B GXM sample is particularly efficient at activating these cellular responses. These immunomodulatory properties correlate with specific serological properties and with a reduced diameter of polysaccharide molecules.

MATERIALS AND METHODS

Fungal strains. The cryptococcal isolates used in this study were selected from the culture collection available in our laboratory. Strains that had previously been more extensively characterized according to their phenotypic characteristics, such as capsule expression, serotype, growth rate, and biochemical properties (6), were used for structural and immunological assays. These samples included *C. neoformans* strains T_1444, HEC3393 (serotype A; clinical isolates), and ATCC 28938 (serotype D; obtained from the American Type Culture Collection, Manassas, VA) and *C. gattii* strains CN23/10.993 (serotype B) and HEC40143 (serotype C) (both environmental isolates). Additional serotype B strains were included in this study based on the results obtained during structural/immunological investigations. These isolates comprised the well-characterized strain R265 (19) and strain ATCC 56990 (American Type Culture Collection). Stock cultures were maintained in Sabouraud dextrose agar under mineral oil and were kept at 4°C.

GXM purification. GXM was isolated as previously described by our group (40). Briefly, *C. neoformans* and *C. gattii* (4×10^9 cells) were suspended in 100 ml of a minimal medium composed of glucose (15 mM), $MgSO_4$ (10 mM), KH_2PO_4 (29.4 mM), glycine (13 mM), and thiamine-HCl (3 μM) (pH 5.5). For all experiments, we used lipopolysaccharide (LPS)-free water and glassware. This suspension was then transferred to a 1,000-ml Erlenmeyer flask and was supplemented with 300 ml of the same medium. Fungal cells were cultivated for 4 days at room temperature, with shaking, and were separated from culture supernatants by centrifugation at 4,000 × *g* (15 min, 4°C). The supernatant fluids were collected and again centrifuged, at 15,000 × *g* (15 min, 4°C), to remove smaller debris. The pellets were discarded, and the resulting supernatant was concentrated approximately 20-fold using an Amicon (Millipore, Danvers, MA) ultrafiltration cell (cutoff, 100 kDa; total capacity, 200 ml) with stirring and Biomax polyethersulfone ultrafiltration discs (diameter, 63.5 mm). A nitrogen (N_2) stream was used as the pressure gas. After supernatant concentration, the viscous layer formed was collected with a cell scraper and was transferred to graduated plastic tubes for measurement of gel volumes. The procedure was repeated at least three times in order to ascertain average volumes. Alternatively, the supernatant fraction passed through the 100-kDa membrane was again concentrated using a 10-kDa filtration disc. The viscous layer was again collected and was used for structural and functional determinations.

ELISA for GXM quantification. The concentrations of GXM in supernatants and concentrated films were determined by capture enzyme-linked immunosorbent assays (ELISA), as previously described (4). Briefly, 96-well polystyrene plates were coated with a goat anti-mouse immunoglobulin M (IgM). After removal of unbound antibodies, a solution of MAb 12A1, an IgM MAb with specificity for GXM, was added to the plate, and this step was followed by blocking with 1% bovine serum albumin (BSA). Supernatants in different dilutions or purified GXM was added to the wells, and the plates were incubated for 1 h at 37°C. The plates were then washed five times with a solution of Tris-buffered saline (TBS) supplemented with 0.1% Tween 20, followed by incubation with MAb 18B7 for 1 h. This antibody is a well-characterized IgG1 that protects mice against lethal challenges with *C. neoformans* and binds to an epitope found in GXM from serotypes A, B, C, and D (3). The plate was again washed and was then incubated with an alkaline phosphatase-conjugated goat anti-mouse IgG1 for 1 h. Reactions were developed after the addition of *p*-nitrophenyl phosphate disodium hexahydrate, and the absorbance at 405 nm was then measured with a microplate reader (TP reader; ThermoPlate). The antibodies for this assay were used at 1 μg/ml.

Monosaccharide analysis. Carbohydrate composition was determined by gas chromatography-mass spectrometry (GC-MS) analysis of the per-*O*-trimethylsilyl (per-*O*-TMS)-derivatized monosaccharides from the polysaccharide films, according to the methodology described by Merkle and Poppe (32). Methyl glycosides were first prepared from the dry sample (0.3 mg) by methanolysis in methanol–1 M HCl at 80°C (18 to 22 h). The sample was then per-O-trimethylsilylated by treatment with Tri-Sil (Pierce) at 80°C (0.5 h). GC-MS analysis of the per-*O*-TMS derivatives was performed on an HP 5890 gas chromatograph interfaced to a 5970 MSD mass spectrometer, using a Supelco DB-1 fused-silica capillary column (length, 30 m; inner diameter, 0.25 mm). The carbohydrate standards used were arabinose, rhamnose, fucose, xylose, glucuronic acid, galacturonic acid, mannose, galactose, glucose, mannitol, dulcitol, and sorbitol.

Transient transfection with TLRs. TLR constructs (16), as well as the β-actin–*Renilla* luciferase construct (49) and the ELAM-1–firefly luciferase reporter construct (45), were kindly provided by Richard Darveau (University of Washington, Seattle). All plasmids used in the transfections were purified using the EndoFree Plasmid Maxi Kit (Qiagen, Valencia, CA) according to the manufacturer's instructions. HEK293A cells (ATCC, Manassas, VA) were cultured in high-glucose Dulbecco's modified Eagle medium (DMEM) (Sigma-Aldrich, St. Louis, MO) supplemented with 10% heat-inactivated fetal bovine serum (FBS) (HyClone, Logan, UT), and the confluent monolayer was harvested by treatment with trypsin-EDTA (Sigma-Aldrich, St. Louis, MO). Cells were seeded in 12-well plates the day before transfection. HEK293A cells were transiently cotransfected with plasmids encoding either mouse TLR2 and TLR1 or TLR2 and TLR6 together with the ELAM-1–firefly luciferase reporter construct and β-actin–*Renilla* luciferase by using Lipofectamine 2000 (Invitrogen, Carlsbad, CA) according to the manufacturer's recommendations. The amount of total DNA per well was normalized to 2 μg by adding an empty vector. On the following day, the transfected cells were plated in 96-well plates.

Luciferase reporter assays for NF-κB activation. Forty-eight hours after transfection, cells were stimulated with purified GXM (1 to 100 μg/ml) for 4 h in DMEM containing 10% FBS. Controls for TLR activation included stimulation of cells with ultrapure LPS from *Escherichia coli* strain 0111:B4 (Invivogen, San Diego, CA), Pam_3Cys-SKKKK (P3C), or FSL-1 (EMC Microcollections, Tübingen, Germany). Then cells were washed once in phosphate-buffered saline (PBS) and were lysed in Passive Lysis Buffer (Promega, Madison, WI). The luciferase activity was measured using the Dual-Luciferase Reporter Assay system (Promega, Madison, WI) according to the manufacturer's instructions. The relative light units (RLU) were quantitated using a Luminoskan luminometer. NF-κB activation is expressed as the ratio of NF-κB-dependent firefly luciferase activity to β-actin-dependent *Renilla* luciferase activity (16). The results are shown as the means and standard deviations of values for triplicate wells.

Nitric oxide production by phagocytes. The murine macrophage-like cell line RAW 264.7 (ATCC) was cultivated under LPS-free conditions in complete DMEM supplemented with 10% fetal calf serum (FCS), 2 mM L-glutamine, 1 mM sodium pyruvate, 10 mg ml/ml gentamicin, MEM Non-Essential Amino Acids Solution (catalog no. 11360; Gibco-Invitrogen), 10 mM HEPES, and 50 mM 2-β-mercaptoethanol at 37°C under a 7.5% CO_2 atmosphere. Murine cells were washed twice in serum-free DMEM and were incubated in fresh medium supplemented with varying concentrations of GXM (1 to 100 μg/ml) for 16 h at 37°C (7.5% CO_2 atmosphere). As a positive control, macrophages were stimulated with 1 μg/ml LPS. Supernatants were then collected and assayed for NO production as described elsewhere (15). Negative controls consisted of supernatants of RAW cells cultivated in a medium containing no GXM. All experiments were performed in triplicate sets.

IF for GXM detection. Antibodies to GXM used in this assay included IgG and IgM. MAbs 12A1 and 13F1 are two clonally related IgMs that differ in fine

specificity and protective efficacy (37, 38). MAb 12A1 is protective and produces annular immunofluorescence (IF) on serotype D *C. neoformans,* while MAb 13F1 is not protective and produces punctate IF. MAb 2D10 (IgM) is also protective in a murine model of cryptococcosis. This antibody reacts with epitopes found throughout the cell wall and capsule of a serotype D strain of *C. neoformans* (13). MAb 18B7 is a protective IgG1 that has been tested as a therapeutic antibody in animals and humans (3, 24). This antibody reacts with all GXM serotypes. *C. neoformans* cells (10^6) were fixed with 4% paraformaldehyde. The cells were further blocked for 1 h in PBS-BSA and were incubated with the MAbs described above (1 μg/ml) for 1 h at room temperature, followed by fluorescein isothiocyanate (FITC)-labeled goat anti-mouse (IgG or IgM) antibodies (Sigma). Yeast cells were finally observed with an Axioplan 2 fluorescence microscope (Zeiss, Germany). Images were acquired using a Color View SX digital camera and were processed with the analySIS software system (Soft Imaging System). Under control conditions, MAbs were replaced by irrelevant isotype-matched antibodies. Exposure times were similar for all conditions.

Biophysical studies. Particle sizes and negative charges of GXM samples were inferred from dynamic light-scattering and zeta potential (ζ) determinations, respectively, by following the methods described by Frases and colleagues (11, 12). For ζ determination, GXM solutions were adjusted to 1 mg/ml in water and were analyzed in a Zeta potential analyzer (ZetaPlus, Brookhaven Instruments Corp., Holtsville, NY). Final values were obtained from the equation $\zeta = (4\pi\eta m)/D$, where D is the dielectric constant of the medium, η is the viscosity, and m is the electrophoretic mobility of the particle. For determination of the effective diameters of GXM molecules, polysaccharide solutions were prepared as described above and were measured by quasi-elastic light scattering in a 90Plus/BI-MAS multiangle particle-sizing analyzer (Brookhaven Instruments Corp., Holtsville, NY). Particle sizes were calculated as described recently (12). Multimodal size distributions analysis of polysaccharide diameters were obtained from of values intensity-weighted sizes fitted to a non-negativity-constrained least-squares (NNLS) algorithm.

Statistics. The existence of significant differences between the different systems analyzed in this study was ascertained using multiple statistical tests. The efficacies of TLR-mediated NF-κB activation and NO production, correlation tests, and biophysical tests were statistically evaluated using Student's *t* test for comparison of two different groups and analysis of variance for comparison of several groups. Statistical tests were performed with GraphPad Prism (version 5.0).

RESULTS

GXM samples from all strains manifest aggregation characteristics. GXM aggregation resulting in the production of purified gels of native polysaccharide was previously demonstrated for a serotype D strain of *C. neoformans* (11, 40). However, it was not clear whether the formation of the viscous polysaccharide films was a strain-specific phenomenon or a general property of cryptococcal strains. Therefore, we evaluated the abilities of polysaccharides from five strains, three *C. neoformans* isolates and two *C. gattii* isolates, to form gels after concentration by ultrafiltration.

Supernatants were obtained from 400-ml cultures containing an initial inoculum of 4×10^9 cells. The final number of cells in each culture differed according to the growth rate of each strain (not shown). Supernatant concentration by ultrafiltration led to the deposition of viscous films on filters for all isolates tested. The volumes of the films were normalized to the final numbers of cells in each culture. This procedure was repeated at least three times for each strain, and different average polysaccharide volumes were generated (Fig. 1A). Next, we analyzed the ability of each isolate to produce extracellular GXM, normalizing the polysaccharide concentration found by ELISA to the final number of cells in the culture. The profile of GXM production by each strain, determined by ELISA (Fig. 1B), resembled very closely that observed for gel formation in the corresponding supernatant. In fact, GXM concentrations in supernatants and gel formation were correlated (R^2, 0.7390; P, 0.0014), as demonstrated in Fig. 1C.

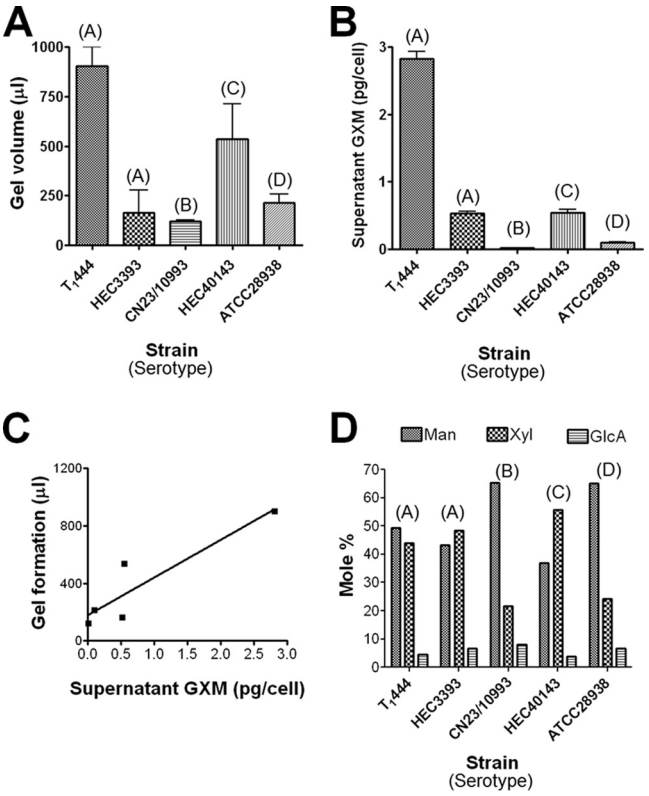

FIG. 1. Quantitative and structural analyses of GXMs from five *Cryptococcus* isolates. GXM was isolated by formation of polysaccharide gels after concentration of culture supernatants of five different isolates of *C. neoformans* and *C. gattii*. (A and B) The volume of gel formation in normalized cultures (A) apparently correlates with the ability of each strain to produce and secrete GXM to the extracellular medium (B). The results are expressed as means ± standard deviations for three different experiments. (C) Correlation properties. (D) Monosaccharide composition of polysaccharides obtained from the five different isolates of *C. neoformans* and *C. gattii*. Monosaccharides were identified by GC-MS; the relative amount of each sugar residue in the polysaccharides is shown as a molar percentage. The serotype of each strain is given in parentheses above the bars.

The sugar composition of each polysaccharide fraction was analyzed by GC-MS (Fig. 1D). After methanolysis of the polysaccharides and per-O-trimethylsilylation of the corresponding products, the resulting monosaccharides were initially identified by their retention times relative to those of standards, followed by structural authentication using MS-MS (not shown). All polysaccharide samples tested had xylose, mannose, and glucuronic acid as major constituents, consistent with the three sugar components of GXM. As previously reported (10, 11), galactose was a trace component of all samples (data not shown). The levels of each GXM building unit differed in polysaccharides from different isolates (Fig. 1D), as normally observed during analysis of different GXM samples. Strains HEC3393 (serotype A) and HEC40143 (serotype C) contained particularly high proportions of xylose, while strains T_1444 (serotype A), CN23/10993 (serotype B), and ATCC 28938 (serotype D) had mannose as their major monosaccharide constituent.

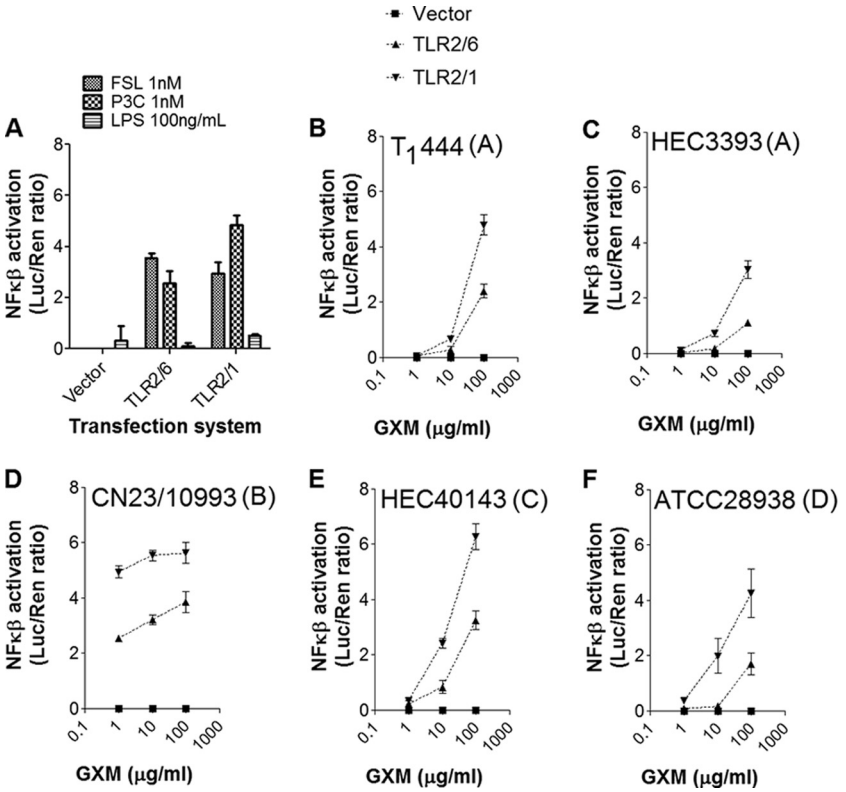

FIG. 2. NF-κB activation in cells expressing TLRs by GXM. (A) Control systems. Pam_3CSK_4 (P_3C) and FSL-1, but not LPS, activated NF-κB nuclear translocation in cells expressing either TLR2/1 or TLR2/6, as expected. Transfection of HEK293A cells with a plasmid containing no TLR-coding sequences (vector) resulted in unresponsiveness. (B to F) Stimulation of HEK293A cells expressing TLR2/1 (inverted triangles) or TLR2/6 (triangles) by GXM samples resulted in dose-dependent NF-κB activation. *Cryptococcus* strains (serotypes) from which each GXM sample was isolated are given at the top of each panel.

NF-κB activation in cells expressing the TLR2/1 or TLR2/6 heterodimer in response to GXM. HEK293A cells expressing either TLR2/1 or TLR2/6 were stimulated with one of the control molecules LPS, P3C, and FSL-1 or with GXM fractions obtained from one of five different *C. neoformans* or *C. gattii* strains (Fig. 2). Transfected cells showed efficient NF-κB activation in response to the synthetic triacylated lipopeptide P3C and to the synthetic diacylated lipopeptide FSL-1, which were used as positive controls for TLR2/1 and TLR2/6 activation, respectively (21). As expected, TLR2/6- or TLR2/1-transfected cells responded very poorly to LPS, the classic TLR4 ligand (18). Also, HEK293A cells transfected with the reporter construct and plasmids containing no TLR-coding sequences (vector) were unresponsive in all cases. All polysaccharide samples induced dose-dependent activation of NF-κB (Fig. 2). NF-κB activation by GXM was always more efficient in cells transfected with the TLR2/1 constructs. Translocation of NF-κB in GXM-treated cells was also more efficient in cells expressing TLR2/1 than in cells transfected with plasmids coding for TLR4/CD14 (data not shown), which were initially described as the receptors involved in GXM-mediated TLR activation (46).

A comparative analysis of the ability of each GXM sample to activate TLR-mediated cellular responses revealed unexpected differences. Although all polysaccharide fractions had the capacity to activate NF-κB in either TLR2/1- or TLR2/6-expressing cells at a concentration of 100 μg/ml, a *C. gattii* polysaccharide sample (serotype B) was significantly more efficient at activating NF-κB than all others (P, <0.0001), with strong signals apparent at 1 and 10 μg/ml (Fig. 3). At 1 μg/ml, NF-κB activation mediated by the serotype B GXM was at least 10-fold higher than that mediated by all other GXM samples for TLR2/1-expressing cells and 6-fold higher for TLR2/6-expressing cells. At 10 μg/ml, the serotype B sample was approximately 2-fold and 4-fold more effective than the other samples in TLR2/1- and TLR2/6-expressing cells, respectively.

NO production in response to GXM stimulation. The GXM samples used for TLR activation were also tested for their abilities to stimulate the production of NO by macrophage-like cells. Exposure of RAW 264.7 cells to GXM from *C. neoformans* cultures resulted in the production of NO at the background level (Fig. 4). Treatment of the phagocytes with *C. gattii* GXM, however, resulted in dose-dependent production of NO. As observed in TLR-based assays, the GXM sample from strain CN23/10993 was the most effective polysaccharide fraction at eliciting NO production.

Structural and serological properties of GXM from *C. neoformans* and *C. gattii*. The differences between the TLR-activating abilities of the various GXM samples led us to investigate the antigenic and physical properties of this polysaccharide set in more detail. The differences in monosaccharide composition between the different samples were not

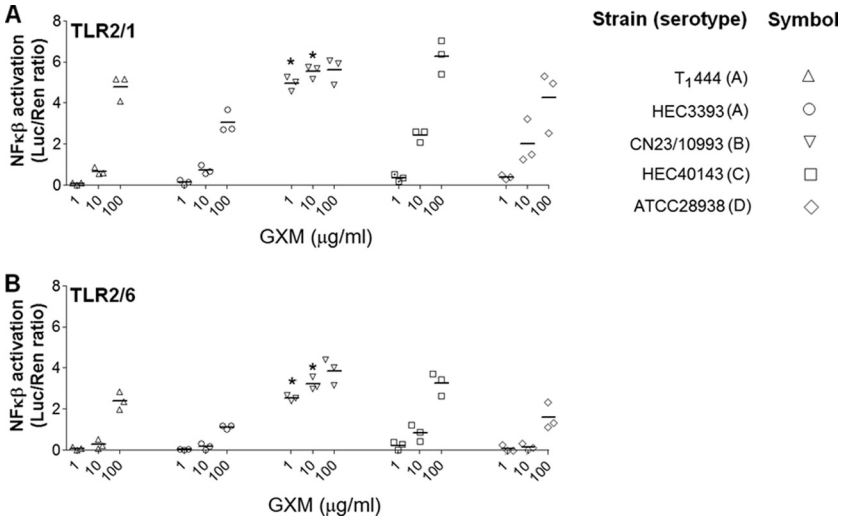

FIG. 3. Comparative analysis of the efficacies of GXM samples in the activation of TLR-mediated NF-κB nuclear translocation. Treatment of HEK293A cells expressing either TLR2/1 (A) or TLR2/6 (B) with GXM revealed that the polysaccharide fractions from strain CN23/10993 were significantly more efficient than all others ($P < 0.0001$) at 1 and 10 μg/ml (asterisks). No significant differences were observed at a higher concentration (100 μg/ml). Strains T_1444, HEC3393, HEC40143, and ATCC 28938 manifested similar efficacies in activating NF-κB nuclear translocation. Strain serotypes are given in the key.

correlated with the ability of GXM to activate cellular responses, since polysaccharide fractions with very similar compositions (strains CN23/10993 and ATCC 28938) manifested different efficacies to induce NO production and TLR2/1- and TLR2/6-mediated NF-κB activation (Fig. 1 to 4).

The negative charge of GXM is an important determinant of function for the capsular polysaccharide in *C. neoformans* (40, 41). Consequently, we determined the zeta potentials of the GXM samples from all the *C. neoformans* and *C. gattii* isolates, which were similar (Table 1). The electrophoretic mobilities of the various GXM preparations were also similar and correlated strictly with zeta potentials (r^2, 0.9992; P, <0.0001). These results therefore suggested that the polysaccharide charge did not affect the activation of NO production and TLR-mediated cellular responses by GXM.

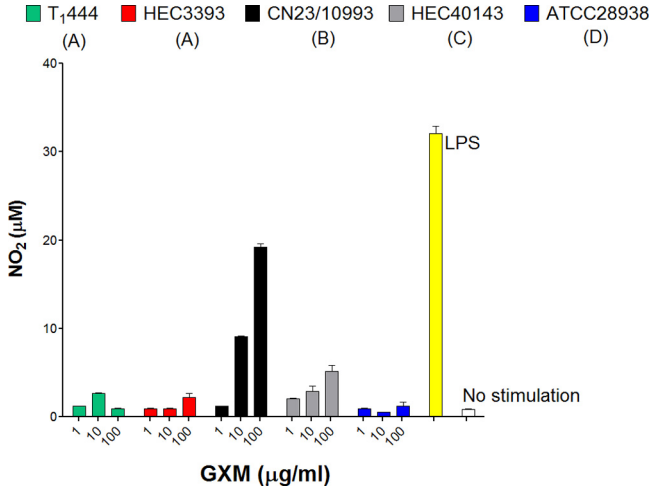

FIG. 4. Comparative analysis of the efficacies of GXM samples in the induction of NO production by macrophages. Polysaccharide fractions from strain CN23/10993 were significantly more efficient at inducing NO production than all others ($P < 0.0001$) at 1, 10, and 100 μg/ml. LPS was used as a positive control for NO production by macrophage-like cells; incubation of the phagocytes in the medium alone (no stimulation) was the negative control. Serotypes are given in parentheses for each strain.

Differences in GXM structure and functions can correlate with reactivity with monoclonal antibodies (42), which led us to evaluate whether the functional discrepancies observed in Fig. 2 to 4 were related to specific serological patterns (Fig. 5). Cells from each of the five *C. neoformans* strains were similarly recognized by MAb 18B7, as demonstrated by immunofluorescence analysis. For all strains, intensities were comparable and the binding pattern was annular. MAbs 2D10, 12A1, and 13F1 produced punctate patterns of reactivity with similar intensities after incubation with strains T_1444, HEC3393, HEC40143, and ATCC 28938. When strain CN23/10993 was used, however, very strong serological reactions were observed with MAb 12A1. In contrast, these cells were not recognized by MAb 13F1.

Effective diameter of GXM. Epitope accessibility in GXM may differ according to the diameter of the molecule (11). In addition, polysaccharide size is a parameter known to influence the activation of TLR2-mediated innate responses (26). We therefore investigated the relationship between NF-κB activa-

TABLE 1. Electronegativities of polysaccharides from five different strains of *C. neoformans* and *C. gattii*

Strain	Serotype	Zeta potential (mV)	Mobility [(μ/s)/(V/cm)]
T_1444	A	−34.50 ± 0.32	−2.70 ± 0.02
HEC3393	A	−33.36 ± 0.51	−2.61 ± 0.04
CN23/10993	B	−33.34 ± 0.21	−2.60 ± 0.02
HEC40143	C	−38.15 ± 0.41	−2.98 ± 0.03
ATCC 28938	D	−34.62 ± 0.45	−2.71 ± 0.04

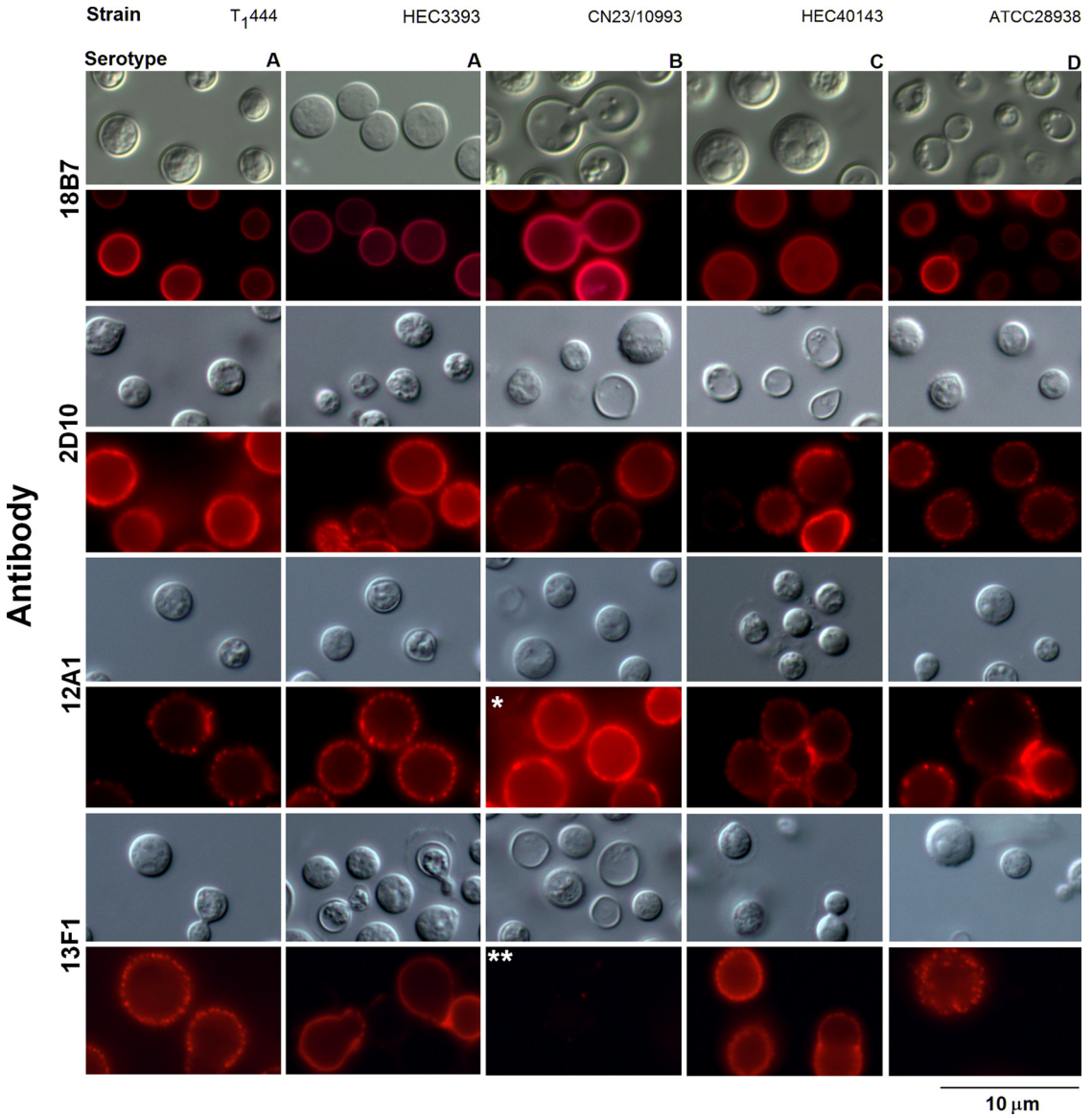

FIG. 5. Reactivities of *C. neoformans* and *C. gattii* isolates with four monoclonal antibodies to GXM. Fungal strains and serotypes are given at the top; antibodies are given on the left. Differential interferential contrast (gray) and fluorescence (red) images are shown. The overreaction of CN23/10993 cells with antibody 12A1 (single asterisk) and their lack of reactivity with antibody 13F1 (double asterisks) are highlighted.

tion and the effective diameter of GXM as measured by dynamic light scattering (Fig. 6). The polysaccharide molecules with the largest diameters came from isolates T_1444 and ATCC 28938 (serotypes A and D, respectively). GXM samples from strains HEC3393 and HEC40143 (serotypes A and C, respectively) showed smaller diameters, which were still larger than that for the polysaccharide isolated from strain CN23/10993 (serotype B). All strains produced polysaccharides with diameters greater than 2 μm, except for strain CN23/10993. Determination of effective diameters by 10 different analyses showed that GXM fractions from the CN23/10993 isolate were significantly shorter (P, <0.0001) than any other polysaccharide. Therefore, the GXM sample containing molecules of the smallest diameter was the most potent polysaccharide in activating the cellular responses in this study.

Smaller GXM fractions from *C. gattii* serotype B strains are more effective at eliciting NO production. In an attempt to establish a correlation between the effective diameters of GXM samples and their abilities to stimulate cellular responses, we fractionated culture supernatants from different cryptococcal isolates. GXM samples were isolated from different strains, including (i) T_1444, due to its ability to produce abundant extracellular polysaccharides with large diameters (Fig. 1 and 6), and (ii) CN23/10993, which was selected on the basis of its ability to produce GXM with apparently higher immunogenicity (Fig. 2 to 4). Two additional serotype B GXMs, from strains R265 and ATCC 56990, were included in this assay for comparative purposes. GXM fractions with molecular masses higher than 100 kDa and in the range of 10 to 100 kDa were obtained by supernatant filtration. The proto-

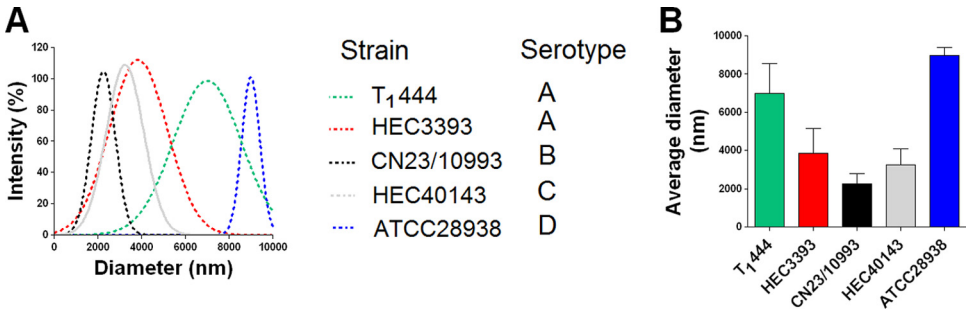

FIG. 6. Diameters of GXM fractions of different isolates of *C. neoformans* and *C. gattii*. (A) Distribution of effective diameters of GXM; (B) average diameters.

type assay used to analyze the relationship between the sizes of GXM samples and their abilities to stimulate cellular responses was NO production by macrophages, since it involves straightforward procedures and simple data interpretation.

Fractionation of the T_1444 supernatant revealed that the high-molecular-mass sample (>100 kDa) induced NO production by phagocytes more efficiently (P, <0.001) than the polysaccharide fraction in the 10- to 100-kDa mass range (Fig. 7A). The opposite pattern was observed for the *C. gattii* samples: all GXM fractions with lower molecular masses were significantly more effective at stimulating the production of NO than the high-molecular-weight polysaccharides (P, <0.0001 for all samples). Again, GXM fractions from strain CN23/10993 were the most effective samples at inducing NO production. The effective diameters of polysaccharides in these fractions were measured by dynamic light scattering, which confirmed that samples with higher molecular masses consisted of molecules of increased dimensions (Fig. 7B). Analysis of serotype B GXM samples (strains CN23/10993, R265, and ATCC 56990) in the 10- to 100-kDa molecular mass range revealed a direct correlation between their abilities to induce NO production and reduced effective diameters (Fig. 7C).

DISCUSSION

Recent studies indicate that the structure of GXM, and consequently its biological functions, differs according to parameters that include molecular mass and effective diameter (11, 12, 40). The functional diversity in cryptococcal polysaccharides is not exclusive to GXM. In fact, it has been reported recently that galactoxylomannan (GalXM) samples from *C. neoformans* are structurally and antigenically variable (8). Therefore, the task of establishing general functions for cryptococcal polysaccharides is complex, since very different characteristics of supposedly similar samples, which presumably reflect differences in polysaccharide structure, have been observed repeatedly in independent studies (8, 11, 40). GXM, for instance, has been classically defined as deleterious to the immune system (51), although it can also activate the host defense (46).

Fungal polysaccharides are potential candidates for activating TLR2-mediated cellular responses. The formation of lipid bodies (multifunctional organelles with critical roles in inflammation) induced by *Histoplasma capsulatum* β-glucan was inhibited in TLR2-deficient mice (47). Chitin, a cell wall structural polysaccharide, has been consistently characterized as a stimulator of TLR2-dependent production of interleukin 17 (IL-17) by macrophages, resulting in the induction of acute inflammation (7).

The ability of *C. neoformans* GXM to activate TLR-mediated innate responses was demonstrated in a number of pre-

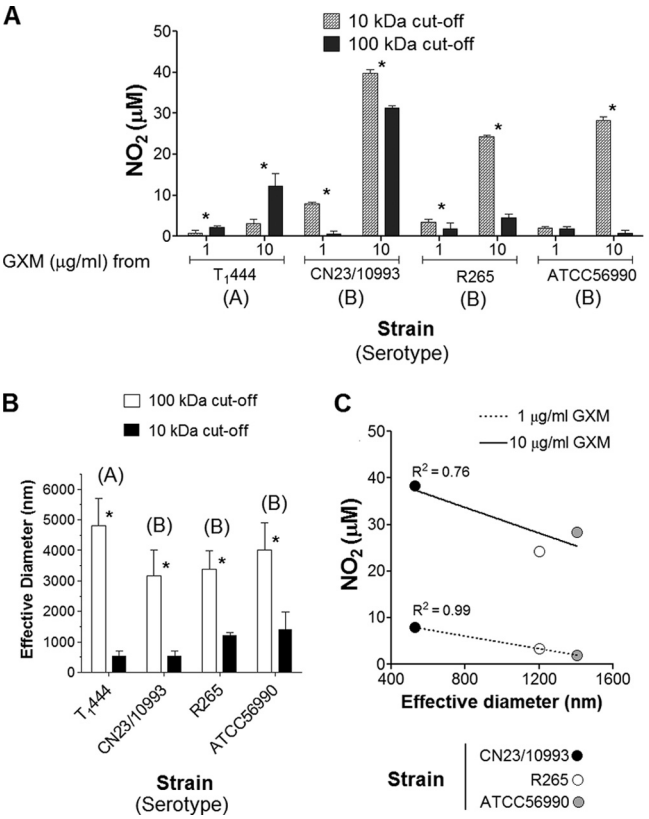

FIG. 7. NO induction by GXM fractions of different molecular masses and effective diameters. (A) Stimulation of macrophage-like cells with the GXM fractions results in differential production of NO. Asterisks indicate significant differences after stimulation of phagocytes with GXM fractions ($P < 0.0001$). (B) Determination of effective diameters of fractions obtained by sequential ultrafiltration through 100-kDa- and 10-kDa-cutoff filtration discs. Asterisks indicate that the differences in effective diameter are statistically significant ($P <$ 0.0001). (C) Correlation analysis of effective diameters of serotype B GXM samples in the 10- to 100-kDa range and their abilities to induce NO.

vious studies (2, 27, 28, 36, 39, 46, 53), but comparable studies have not been carried out for *C. gattii* polysaccharides. TLRs and the CD14 receptor function as pattern recognition receptors for GXM (27, 28, 36, 44, 46, 53). The binding of GXM to TLR4 has been reported to result in the translocation of NF-κB to the nucleus in an incomplete process that does not induce the activation of mitogen-activated protein kinase pathways or the release of tumor necrosis factor alpha (TNF-α) (46). TLR4 was also implicated in the cellular uptake (34) and tissue distribution (52) of GXM. However, the roles of TLR2 and other TLRs in the immune response to GXM remain poorly understood. In the present study, we determined that the hydrodynamic size of GXM fractions is correlated with their ability to stimulate NO production by macrophages and to activate NF-κB in a TLR2-dependent manner. In fact, all GXM fractions stimulated the activation of NF-κB in HEK293A cells transiently transfected with TLR2/TLR6 or TLR2/TLR1 constructs. This response was always more intense in cells expressing the TLR2/1 construct than in those expressing the TLR2/6 construct. In all systems, the highest levels of NF-κB activation were obtained when transfected HEK293A cells were exposed to a serotype B GXM from a *C. gattii* strain.

To understand the structural characteristics responsible for NO and TLR activation, we evaluated several GXM parameters. The ability of GXM to induce NO production and the TLR-mediated response in transfected HEK293A cells was not an intraspecies property and did not depend on sugar composition, so other parameters were evaluated. Differences in antibody reactivity can imply differences in GXM structure (11), which also denote functional specificity (20). In this study, we found that the serological characteristics revealed by the binding of MAbs were similar in all strains, except for the *C. gattii* strain CN23/10993. Those cells showed strong reactivity with the protective IgM 12A1 but did not react with the clonally related nonprotective MAb 13F1. This observation is consistent with, and reflective of, the fact that MAbs 12A1 and 13F1 bind to different epitopes. In a recent study, it was suggested that antibody reactivity is influenced by the diameter of GXM (10), which led us to the inference that the effective diameters of the polysaccharide samples used in this study could also be related to the functionality of GXM.

Immunological studies with chitin have shown that large polysaccharide polymers are biologically inert, while their fragments are efficient regulators of TLR2-mediated innate immune responses (7, 25, 26). Human cryptococcosis caused by *C. gattii* is known to produce strong inflammatory responses in the lung, whereas the *C. neoformans* varieties often trigger little or no inflammation (49). Consequently, the result that serotype B GXM samples were more potent activators of cellular responses raises the tantalizing possibility that a correlation might exist between the activation of host cells and the type of granulomatous response made. In our model, the most effective GXM sample in activating cellular responses had the smallest effective diameter, a result that echoed previous findings with chitin (7, 25, 26). Using the model of NO production by macrophages after exposure to the serotype B GXM, we observed that polysaccharides with reduced dimensions induced a stronger cellular response, a property that was exclusive to serotype B GXM samples. NO production by macrophages is involved in both antimicrobial responses and the mediation of inflammation, illustrating the complex effects of GXM on host immune function. Given that our studies compared GXM preparations standardized by mass/volume and that smaller fibers have lower molecular masses, it is possible that the effects measured here reflect differences in the molarity of the GXM. Nevertheless, we urge caution in attributing these effects to simple differences in molarity, since interactions between polysaccharides and their receptors are likely to involve repeating structural motifs in polysaccharide molecules such that avidity considerations could be dominant. Furthermore, we note that immunological studies routinely measure effects using polysaccharide concentrations standardized by mass/volume, and consequently, this approach is experimentally relevant, especially for literature comparisons.

The cryptococcal capsule enlarges during infection, which is essential for virulence (54). A linear correlation between the effective diameter of GXM and the microscopic capsular diameter has recently been demonstrated (12), suggesting that the synthesis of large-diameter polysaccharides is essential for capsule enlargement. In our model, strain CN23/10993 produced GXM molecules with the lowest effective diameters and had the smallest capsular dimension (data not shown). The combination of the ability of GXM to modulate cellular responses and the capacity of *C. neoformans* to produce large GXM molecules and capsules may have a direct impact on fungal virulence. *C. neoformans* isolates producing large GXM molecules would be more efficient at producing capsules with increased dimensions, which are generally associated with pathogenic potential (54). On the other hand, isolates producing smaller GXM molecules, according to our current results, would manifest a potentially enhanced ability to activate some mechanisms of the immune response. Considering that the cryptococcal capsule also protects the fungus from a number of host antifungal mechanisms, a combination of smaller GXM molecules and the formation of a capsular network with reduced dimensions would favor the host defense by multiple mechanisms. We therefore suggest that the synthesis of capsular structures with reduced dimensions could have protean effects on the pathogenic capacities of cryptococcal strains, ranging from increased susceptibility to oxidative fluxes and phagocytosis to the production of molecules with an enhanced ability to activate host defenses. These observations suggest a mechanistic explanation for the consistent observation that strains with small capsules elicit more inflammation than those with large capsules (43). Furthermore, the higher NO-inducing activity associated with *C. gattii* polysaccharides, which correlates with smaller GXM diameters, suggests an explanation for the consistent observation of stronger granulomatous responses in cryptococcosis caused by this species (33, 43, 48).

ACKNOWLEDGMENTS

M.L.R. and L.N. are supported by grants from the Coordenação de Aperfeiçoamento de Pessoal de Nível Superior (CAPES, Brazil), Conselho Nacional de Desenvolvimento Científico e Tecnológico (CNPq, Brazil), Fundação de Amparo a Pesquisa do Estado de São Paulo (FAPESP, Brazil), and Fundação de Amparo a Pesquisa do Estado do Rio de Janeiro (FAPERJ, Brazil). A.C. is supported by NIH grants AI033142, AI033774, AI052733, and HL059842. I.C.A. is supported by NIH/NCRR grant 5G12RR008124-16A1. L.L.N. is partially supported by the Cotton Memorial Scholarship (University of Texas at El Paso

[UTEP]), Good Neighbor Scholarship (UTEP), and Florence Terry Griswold Scholarship-I (PARTT). R.J.B.C. is supported by the Training Program in Cellular and Molecular Biology and Genetics, T32 GM007491. Carbohydrate analyses were performed at the Complex Carbohydrate Research Center, University of Georgia—Athens, which is supported in part by the Department of Energy-funded (DE-FG-9-93ER-20097) Center for Plant and Microbial Complex Carbohydrates. TLR experiments were partly carried out at the Biomolecule Analysis (BACF) and Cell Culture and High Throughput Screening core facilities, Border Biomedical Research Center (BBRC), UTEP, supported by NIH/NCRR grants 5G12RR008124-16A1 and 3G12RR008124-16A1S1 (BACF).

We thank Jorge José Jó B. Ferreira and Rosana Puccia for helpful discussions and Natalia Freire for help with GXM fractionation. We are also indebted to Sonia Rozental and Marilene Vainstein for the gifts of strains ATCC 56990 and R265.

REFERENCES

1. **Bicanic, T., and T. S. Harrison.** 2004. Cryptococcal meningitis. Br. Med. Bull. **72:**99–118.
2. **Biondo, C., A. Midiri, L. Messina, F. Tomasello, G. Garufi, M. R. Catania, M. Bombaci, C. Beninati, G. Teti, and G. Mancuso.** 2005. MyD88 and TLR2, but not TLR4, are required for host defense against Cryptococcus neoformans. Eur. J. Immunol. **35:**870–878.
3. **Casadevall, A., W. Cleare, M. Feldmesser, A. Glatman-Freedman, D. L. Goldman, T. R. Kozel, N. Lendvai, J. Mukherjee, L. A. Pirofski, J. Rivera, A. L. Rosas, M. D. Scharff, P. Valadon, K. Westin, and Z. Zhong.** 1998. Characterization of a murine monoclonal antibody to Cryptococcus neoformans polysaccharide that is a candidate for human therapeutic studies. Antimicrob. Agents Chemother. **42:**1437–1446.
4. **Casadevall, A., J. Mukherjee, and M. D. Scharff.** 1992. Monoclonal antibody based ELISAs for cryptococcal polysaccharide. J. Immunol. Methods **154:** 27–35.
5. **Chiapello, L. S., J. L. Baronetti, A. P. Garro, M. F. Spesso, and D. T. Masih.** 2008. Cryptococcus neoformans glucuronoxylomannan induces macrophage apoptosis mediated by nitric oxide in a caspase-independent pathway. Int. Immunol. **20:**1527–1541.
6. **Collopy-Junior, I., F. F. Esteves, L. Nimrichter, M. L. Rodrigues, C. S. Alviano, and J. R. Meyer-Fernandes.** 2006. An ectophosphatase activity in Cryptococcus neoformans. FEMS Yeast Res. **6:**1010–1017.
7. **Da Silva, C. A., D. Hartl, W. Liu, C. G. Lee, and J. A. Elias.** 2008. TLR-2 and IL-17A in chitin-induced macrophage activation and acute inflammation. J. Immunol. **181:**4279–4286.
8. **De Jesus, M., S. K. Chow, R. J. Cordero, S. Frases, and A. Casadevall.** 8 January 2010. Galactoxylomannans from Cryptococcus neoformans varieties neoformans and grubii are structurally and antigenically variable. Eukaryot. Cell. doi:10.1128/EC.00268-09.
9. **Doering, T. L.** 2000. How does Cryptococcus get its coat? Trends Microbiol. **8:**547–553.
10. **Fonseca, F. L., S. Frases, A. Casadevall, O. Fischman-Gompertz, L. Nimrichter, and M. L. Rodrigues.** 2009. Structural and functional properties of the Trichosporon asahii glucuronoxylomannan. Fungal Genet. Biol. **46:**496–505.
11. **Frases, S., L. Nimrichter, N. B. Viana, A. Nakouzi, and A. Casadevall.** 2008. Cryptococcus neoformans capsular polysaccharide and exopolysaccharide fractions manifest physical, chemical, and antigenic differences. Eukaryot. Cell **7:**319–327.
12. **Frases, S., B. Pontes, L. Nimrichter, N. B. Viana, M. L. Rodrigues, and A. Casadevall.** 2009. Capsule of Cryptococcus neoformans grows by enlargement of polysaccharide molecules. Proc. Natl. Acad. Sci. U. S. A. **106:**1228–1233.
13. **García-Rivera, J., Y. C. Chang, K. J. Kwon-Chung, and A. Casadevall.** 2004. Cryptococcus neoformans CAP59 (or Cap59p) is involved in the extracellular trafficking of capsular glucuronoxylomannan. Eukaryot. Cell **3:**385–392.
14. **Gautam, J. K., Ashish, L. D. Comeau, J. K. Krueger, and M. F. Smith, Jr.** 2006. Structural and functional evidence for the role of the TLR2 DD loop in TLR1/TLR2 heterodimerization and signaling. J. Biol. Chem. **281:**30132–30142.
15. **Green, L. C., D. A. Wagner, J. Glogowski, P. L. Skipper, J. S. Wishnok, and S. R. Tannenbaum.** 1982. Analysis of nitrate, nitrite, and [^{15}N]nitrate in biological fluids. Anal. Biochem. **126:**131–138.
16. **Hajjar, A. M., D. S. O'Mahony, A. Ozinsky, D. M. Underhill, A. Aderem, S. J. Klebanoff, and C. B. Wilson.** 2001. Functional interactions between toll-like receptor (TLR) 2 and TLR1 or TLR6 in response to phenol-soluble modulin. J. Immunol. **166:**15–19.
17. **Jin, M. S., S. E. Kim, J. Y. Heo, M. E. Lee, H. M. Kim, S. G. Paik, H. Lee, and J. O. Lee.** 2007. Crystal structure of the TLR1-TLR2 heterodimer induced by binding of a tri-acylated lipopeptide. Cell **130:**1071–1082.
18. **Jin, M. S., and J. O. Lee.** 2008. Structures of the toll-like receptor family and its ligand complexes. Immunity **29:**182–191.
19. **Kidd, S. E., F. Hagen, R. L. Tscharke, M. Huynh, K. H. Bartlett, M. Fyfe, L. Macdougall, T. Boekhout, K. J. Kwon-Chung, and W. Meyer.** 2004. A rare genotype of Cryptococcus gattii caused the cryptococcosis outbreak on Vancouver Island (British Columbia, Canada). Proc. Natl. Acad. Sci. U. S. A. **101:**17258–17263.
20. **Kozel, T. R., S. M. Levitz, F. Dromer, M. A. Gates, P. Thorkildson, and G. Janbon.** 2003. Antigenic and biological characteristics of mutant strains of Cryptococcus neoformans lacking capsular O acetylation or xylosyl side chains. Infect. Immun. **71:**2868–2875.
21. **Krishnegowda, G., A. M. Hajjar, J. Zhu, E. J. Douglass, S. Uematsu, S. Akira, A. S. Woods, and D. C. Gowda.** 2005. Induction of proinflammatory responses in macrophages by the glycosylphosphatidylinositols of Plasmodium falciparum: cell signaling receptors, glycosylphosphatidylinositol (GPI) structural requirement, and regulation of GPI activity. J. Biol. Chem. **280:** 8606–8616.
22. **Kumar, H., T. Kawai, and S. Akira.** 2009. Toll-like receptors and innate immunity. Biochem. Biophys. Res. Commun. **388:**621–625.
23. **Kwon-Chung, K. J., and A. Varma.** 2006. Do major species concepts support one, two or more species within Cryptococcus neoformans? FEMS Yeast Res. **6:**574–587.
24. **Larsen, R. A., P. G. Pappas, J. Perfect, J. A. Aberg, A. Casadevall, G. A. Cloud, R. James, S. Filler, and W. E. Dismukes.** 2005. Phase I evaluation of the safety and pharmacokinetics of murine-derived anticryptococcal antibody 18B7 in subjects with treated cryptococcal meningitis. Antimicrob. Agents Chemother. **49:**952–958.
25. **Lee, C. G.** 2009. Chitin, chitinases and chitinase-like proteins in allergic inflammation and tissue remodeling. Yonsei Med. J. **50:**22–30.
26. **Lee, C. G., C. A. Da Silva, J. Y. Lee, D. Hartl, and J. A. Elias.** 2008. Chitin regulation of immune responses: an old molecule with new roles. Curr. Opin. Immunol. **20:**684–689.
27. **Levitz, S. M.** 2002. Receptor-mediated recognition of Cryptococcus neoformans. Nippon Ishinkin Gakkai Zasshi **43:**133–136.
28. **Levitz, S. M.** 2004. Interactions of Toll-like receptors with fungi. Microbes Infect. **6:**1351–1355.
29. **Liang, S., K. B. Hosur, S. Lu, H. F. Nawar, B. R. Weber, R. I. Tapping, T. D. Connell, and G. Hajishengallis.** 2009. Mapping of a microbial protein domain involved in binding and activation of the TLR2/TLR1 heterodimer. J. Immunol. **182:**2978–2985.
30. **McClelland, E. E., P. Bernhardt, and A. Casadevall.** 2005. Coping with multiple virulence factors: which is most important? PLoS Pathog. **1:**e40.
31. **McFadden, D., O. Zaragoza, and A. Casadevall.** 2006. The capsular dynamics of Cryptococcus neoformans. Trends Microbiol. **14:**497–505.
32. **Merkle, R. K., and I. Poppe.** 1994. Carbohydrate composition analysis of glycoconjugates by gas-liquid chromatography/mass spectrometry. Methods Enzymol. **230:**1–15.
33. **Mitchell, D. H., T. C. Sorrell, A. M. Allworth, C. H. Heath, A. R. McGregor, K. Papanaoum, M. J. Richards, and T. Gottlieb.** 1995. Cryptococcal disease of the CNS in immunocompetent hosts: influence of cryptococcal variety on clinical manifestations and outcome. Clin. Infect. Dis. **20:**611–616.
34. **Monari, C., F. Bistoni, A. Casadevall, E. Pericolini, D. Pietrella, T. R. Kozel, and A. Vecchiarelli.** 2005. Glucuronoxylomannan, a microbial compound, regulates expression of costimulatory molecules and production of cytokines in macrophages. J. Infect. Dis. **191:**127–137.
35. **Monari, C., F. Bistoni, and A. Vecchiarelli.** 2006. Glucuronoxylomannan exhibits potent immunosuppressive properties. FEMS Yeast Res. **6:**537–542.
36. **Monari, C., E. Pericolini, G. Bistoni, A. Casadevall, T. R. Kozel, and A. Vecchiarelli.** 2005. Cryptococcus neoformans capsular glucuronoxylomannan induces expression of Fas ligand in macrophages. J. Immunol. **174:**3461–3468.
37. **Mukherjee, J., G. Nussbaum, M. D. Scharff, and A. Casadevall.** 1995. Protective and nonprotective monoclonal antibodies to Cryptococcus neoformans originating from one B cell. J. Exp. Med. **181:**405–409.
38. **Mukherjee, J., M. D. Scharff, and A. Casadevall.** 1992. Protective murine monoclonal antibodies to Cryptococcus neoformans. Infect. Immun. **60:**4534–4541.
39. **Nakamura, K., K. Miyagi, Y. Koguchi, Y. Kinjo, K. Uezu, T. Kinjo, M. Akamine, J. Fujita, I. Kawamura, M. Mitsuyama, Y. Adachi, N. Ohno, K. Takeda, S. Akira, A. Miyazato, M. Kaku, and K. Kawakami.** 2006. Limited contribution of Toll-like receptor 2 and 4 to the host response to a fungal infectious pathogen, Cryptococcus neoformans. FEMS Immunol. Med. Microbiol. **47:**148–154.
40. **Nimrichter, L., S. Frases, L. P. Cinelli, N. B. Viana, A. Nakouzi, L. R. Travassos, A. Casadevall, and M. L. Rodrigues.** 2007. Self-aggregation of Cryptococcus neoformans capsular glucuronoxylomannan is dependent on divalent cations. Eukaryot. Cell **6:**1400–1410.
41. **Nosanchuk, J. D., and A. Casadevall.** 1997. Cellular charge of Cryptococcus neoformans: contributions from the capsular polysaccharide, melanin, and monoclonal antibody binding. Infect. Immun. **65:**1836–1841.
42. **Nussbaum, G., W. Cleare, A. Casadevall, M. D. Scharff, and P. Valadon.** 1997. Epitope location in the Cryptococcus neoformans capsule is a determinant of antibody efficacy. J. Exp. Med. **185:**685–694.

43. **Perfect, J. R., and A. Casadevall.** 2002. Cryptococcosis. Infect. Dis. Clin. North Am. **16:**837–874.
44. **Roeder, A., C. J. Kirschning, R. A. Rupec, M. Schaller, and H. C. Korting.** 2004. Toll-like receptors and innate antifungal responses. Trends Microbiol. **12:**44–49.
45. **Schindler, U., and V. R. Baichwal.** 1994. Three NF-κB binding sites in the human E-selectin gene required for maximal tumor necrosis factor alpha-induced expression. Mol. Cell. Biol. **14:**5820–5831.
46. **Shoham, S., C. Huang, J. M. Chen, D. T. Golenbock, and S. M. Levitz.** 2001. Toll-like receptor 4 mediates intracellular signaling without TNF-α release in response to Cryptococcus neoformans polysaccharide capsule. J. Immunol. **166:**4620–4626.
47. **Sorgi, C. A., A. Secatto, C. Fontanari, W. M. Turato, C. Belanger, A. I. de Medeiros, S. Kashima, S. Marleau, D. T. Covas, P. T. Bozza, and L. H. Faccioli.** 2009. Histoplasma capsulatum cell wall β-glucan induces lipid body formation through CD18, TLR2, and dectin-1 receptors: correlation with leukotriene B4 generation and role in HIV-1 infection. J. Immunol. **182:** 4025–4035.
48. **Speed, B., and D. Dunt.** 1995. Clinical and host differences between infections with the two varieties of Cryptococcus neoformans. Clin. Infect. Dis. **21:**28–34.
49. **Sweetser, M. T., T. Hoey, Y. L. Sun, W. M. Weaver, G. A. Price, and C. B. Wilson.** 1998. The roles of nuclear factor of activated T cells and ying-yang 1 in activation-induced expression of the interferon-gamma promoter in T cells. J. Biol. Chem. **273:**34775–34783.
50. **Triantafilou, M., F. G. Gamper, R. M. Haston, M. A. Mouratis, S. Morath, T. Hartung, and K. Triantafilou.** 2006. Membrane sorting of toll-like receptor (TLR)-2/6 and TLR2/1 heterodimers at the cell surface determines heterotypic associations with CD36 and intracellular targeting. J. Biol. Chem. **281:**31002–31011.
51. **Vecchiarelli, A.** 2007. Fungal capsular polysaccharide and T-cell suppression: the hidden nature of poor immunogenicity. Crit. Rev. Immunol. **27:**547–557.
52. **Yauch, L. E., M. K. Mansour, and S. M. Levitz.** 2005. Receptor-mediated clearance of Cryptococcus neoformans capsular polysaccharide in vivo. Infect. Immun. **73:**8429–8432.
53. **Yauch, L. E., M. K. Mansour, S. Shoham, J. B. Rottman, and S. M. Levitz.** 2004. Involvement of CD14, toll-like receptors 2 and 4, and MyD88 in the host response to the fungal pathogen Cryptococcus neoformans in vivo. Infect. Immun. **72:**5373–5382.
54. **Zaragoza, O., M. L. Rodrigues, M. De Jesus, S. Frases, E. Dadachova, and A. Casadevall.** 2009. The capsule of the fungal pathogen Cryptococcus neoformans. Adv. Appl. Microbiol. **68:**133–216.

Editor: G. S. Deepe, Jr.